www.ijselam.com editor@ijselam.com

International Journal of Science, Engineering, Law, Arts and Management (IJSELAM)

e-ISSN:XXXX - XXXX

VOLUME 1, ISSUE 1, MARCH 2026

Ahmed Mohmed Ibrahim Suliman Badria Ali Gismalla,
Mohammed El Amin Ahmed Babikir, Mohammed Fatur Zaid

Generation of 3D Models from Twin-Low-Oblique Photographs without Ground Control

Ahmed Mohmed Ibrahim Suliman[1], **Badria Ali Gismalla**[1], **Mohammed El amin Ahmed Babikir**[2], **Mohammed Fatur Zaid**[3]

[1،2 ،3] Department of Surveying, College of Engineering, Khartoum, Khartoum State, Sudan.

Email: ibrahimaamaa@gmail.com

ABSTRACT

In recent last few years, there was a tremendously increasing use of digital photogrammetry especially that which uses oblique images due to increasing needs for more details extracted from aerial images. Oblique imagery has an ability to reduce efforts and budget that are consumed by conventional photogrammetry.

This paper presents some ideas about the kinds of products that can be obtained from an oblique photography, such as referenced orthomosaics and Digital Elevation Models (DEMs) which can be used to generate three dimensional models. The results obtained from the study showed that oblique imageries can be satisfactorily used to determine target points without any need for the generally expensive and time-consuming ground control.

Keywords *— Oblique Images, Digital Photogrammetry, Nadir Images, Point Cloud, Target Points, Stereoscopic Viewing.*

1. Introduction

Photogrammetry, the use of photography for surveying, primarily facilitates the production of maps and geographic data bases from aerial photographs. Along with Remote Sensing (RS), it represents the principal means of generating data for Geographic Information Systems (GIS). Photogrammetry has undergone a remarkable revolution in recent years with its transformation into digital photogrammetry. First, the distinction between photogrammetry, RS, Geodesy, and GIS are rapidly disappearing, as data can now be collected digitally from the camera onboard an aeroplane to the GIS end-user. Second, the benefits of digital photogrammetric workstations have increased dramatically. The comprehensive use of digital instruments and tools, together with automation of all processes, have significantly reduced both costs and processing time. Digital aerial cameras have become available, and the introduction of more and more new digital tools allow the work to be carried out with simplicity and without the need for skilled operators. Engineers benefiting from photogrammetry can now carry out their own work without any need for the help of professional photogrammetrists.

Photogrammetry may be considered as a measuring technique that allows modelling of a three dimensional space using two dimensional images. Of course, this is perfectly suitable for the case where one uses photographic pictures, but this is still the case when any other type of a two-dimensional acquisition device is used, a radar or a scanning device for example. Generally, the photogrammetric process is basically independent of the image type. (Kasser and Egels, 2004).

In general, almost all processes in photogrammetric solutions need Ground Control Points (GCPs).

These are ground points having known ground coordinates. The provision of such control is time consuming and very expensive. It financially constitutes the major cost in any photogrammetric project.

1.1 Geometric Principles

Obviously, from a single photograph (two-dimensional plane) we can only get two-dimensional coordinates. Therefore, if we need three-dimensional coordinates, we have to find a way how to get the third dimension. The so-called stereoscopic viewing principle is used to get three-dimensional information in photogrammetry. If we have two, or more, photographs for the same object but taken from different positions, we may easily calculate the three-dimensional coordinates of any point appearing in the overlapping area. i.e points appearing in consecutive photographs.

Each point on the terrain surface (object point) is represented in at least two photographs. If we know, or able to construct, all geometric parameters of the situation at the instant of exposure, then we can calculate the three-dimensional coordinates (X, Y, Z) of any point by setting up equations of the rays emerging from the ground point to the camera lens and thereafter calculating their intersection. This process is actually the main task of photogrammetry.

The accuracy of the result depends mainly on the intersection angle of the two rays at the point. The smaller this angle is, the lesser will be the accuracy. Even very small errors in an image position of a point will lead to a large error, especially in the Z-coordinate (height), when the angle is very small. In fact, this is the main reason why wide-angle cameras are preferred over normal and narrow-angle cameras (Linder, 2006).

1.2 Oblique Images

Oblique images are taken such that orientation of the optical axis is intentionally tilted from the vertical (i. e. from nadir direction). If the horizon is visible, the image is called high oblique or, otherwise, low oblique. Oblique images are usually captured by multiple lens systems. These systems consist of two, or more, lenses mounted on the same camera body or two, or more, cameras mounted on an array in such a way that angles between their optical are kept fixed. The shutters are usually synchronized for the purpose of obtaining exposures at the same instant. The accuracy largely depends on how well the optical axes have been calibrated and retained (GIM International, 2014).

Oblique airborne multi-camera systems are becoming a standard sensor technology across a growing Geo-spatial market with multiple applications next to the more standard vertical photography and its derivatives; Digital Surface Models (DSMs), orthophotographs, and maps. In line with automation of photogrammetric workflow, digital camera technology has leveled up and the definition of large-format has been pushed forward.

The use of oblique imagery has become a standard for many civil and mapping applications. The indisputable advantage of oblique photography lies in its simplicity of interpretation and understanding its content for inexperienced users allowing their use in very different applications, such as building detection and reconstruction, building structural damage classification, road land updating and administration services, ….etc. (Rupnick, Nex and Remondino, 2014).

Oblique images are generally used for various reasons. These include:

- There is a strong movement towards combining traditional nadir images (vertical images) with oblique images acquired at high angles to build 3D models of cities with the texture of building walls taken from oblique photographs.

For non-specialists in emergency services e. g. police, the combination of oblique and nadir images:

- Improves their interpretation while a specialized software allows simple measurements on an oblique photograph to be carried out with ease and simplicity.
- Part of current interest in multiple oblique camera configurations stems from the limitations in the size of current Charged Coupled Devices (CCDs) and Complementary Metal Oxide Semiconductor (CMOS) arrays for digital cameras; hence the use of multiple oblique cameras by a number of system suppliers to increase ground area that can be covered from a single exposure station.
- Besides the increase in coverage area of rectangular or square format digital frame photographs, there is a long-standing requirement on the part of military air forces to obtain the widest possible cross-track angular coverage using fans of oblique cameras for reconnaissance purposes.
- Apart from the multi-photo and multi-camera aspects of oblique aerial photography, the oblique imaging configuration is also of increasing importance for both surveillance and visualization purposes with the acquisition of both single and multiple digital images from both manned and unmanned platforms, often from low altitudes (Petrie, 2008).

1.3 Twin Oblique Cameras

Twin oblique film cameras have been extensively used in the past to provide an increased coverage either cross-track or along-track. At recent times, there is an increasing use of twin oblique digital frame cameras to provide increased cross- track coverage and more details about heights of terrain and buildings in urban areas. Two frames can be merged into one large frame in order to double the sensor size and, therefore, a larger coverage as a result.

1.4 Airsoft Photo Scan (APS)

Airsoft Photo Scan is a stand-alone software product that performs photogrammetric processing of digital images and generates 3D spatial data to be used in GIS applications, cultural heritage documentation, and visual effects production as well as indirect measurements of objects of various shapes.

Implementing techniques of digital photogrammetry integrated with computer vision methods results in a smart automated processing system that, on the one hand, can be managed by a non-specialist in the field of photogrammetry. On the other hand, it has a lot to offer to a specialist who can adjust the workflow to many specific tasks and different data types.

The software allows to efficiently reduce computation time while working with a huge amount of different data, making operations with large data volume very smooth in a compatible GIS. It has proved to be a professional level post-processing tool capable of dense point cloud generation and classification for further detailed calculations of DSMs, Digital Terrain Models (DTMs) and high resolution orthomosaics export. In simple, Agisoft Photo Scan is a solution for automatic generation of dense point cloud, textured polygonal models, Geo-referenced orthomosaics and DSMs and/or DTMs from still images. For more detailed information about this, the reader is recommended to visit www.agisoft.com.

2. Methods and Materials

In the following paragraphs, the methodology adopted in this research is presented.

2.1 The Study Area

A selected area in Khartoum (Sudan) metropolitan area between top: 1,727,358.653m N (left), 445,136.723m E(right), 450,432.128m; bottom: 1,723,132.858N was used in this study (Figure (1))

The area falls in Almugran (an Arabic word meaning junction of two, or more, water courses such as rivers) area where the Blue Nile and White Nile meet to form the River Nile. The area is known by its high tower buildings and covers 14 square kilometers approximately.

Figure (1) The Study Area

2.2 The Imaging System Used

The imaging system used consists of two digital cameras mounted on an aero-stablizer linked with a Global Navigation Satellite System (GNSS) integrated with an Inertial Measurement Unit (IMU) sensor that provides coordinates of camera stations, camera height above mean sea level and exterior orientation rotation parameters. These types of camera systems are not really oblique, they, rather, are near vertical; as a result they do not show building facades. However, they can be adapted to become complete oblique systems.

2.3 Photographic Coverage

The area is covered by four strips (flight lines) each of which consists of 10 camera stations or, as sometimes called, exposure stations as shown in Figure (2). These actually represent positions of the camera at the moment of exposure. At each one of these 40 camera stations, two overlapping images were taken with an overlap of 20%. The planned Ground Sample Distance (GSD) is 85 mm with over and side laps of 60% and 35% respectively.

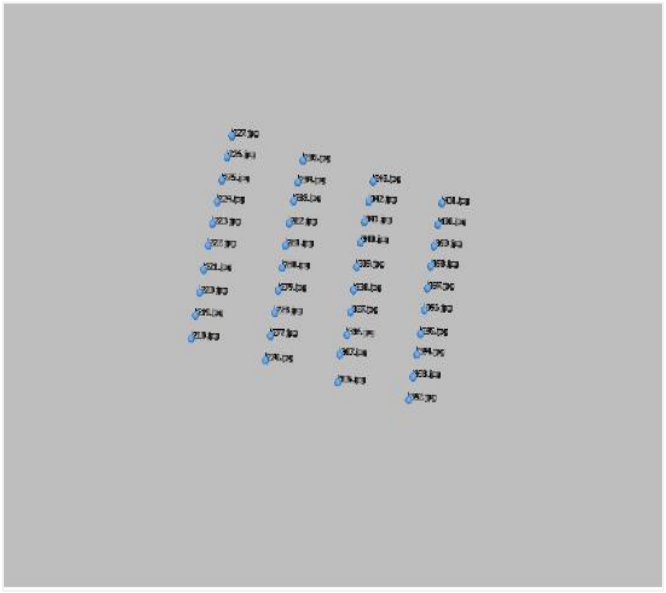

Figure (2) Image Stations

2.4. Image Enhancement

The images were enhanced and brought into a suitable format after which GNSS and IMU were adjusted to match each image with the corresponding coordinates and exterior orientation angular parameters. The chosen photographs are then joined together to form a block of photographs as shown in Figure (3).

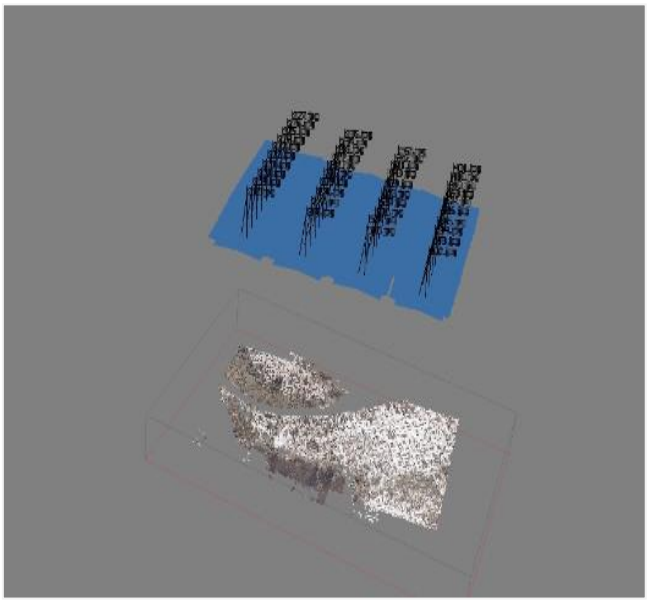

Figure (3) Joined Camera Stations and Flight Altitudes

3. Modeling and Analysis

A dense point cloud model was generated based on the estimated camera positions. The program calculates depth (height) information for each camera to be combined into a single dense point cloud. The result is shown in Figure (4).

After dense point cloud construction, it is possible to generate a polygonal mesh model based on the dense cloud data. A 3D model texture is then generated to determine how the object texture will be. This step helps to obtain optimal texture packing and, consequently, better visual quality of the final model. It depends on the appearance of building facades appearing on the images which requires an increase in the over laps between images and the camera angle. This is not really needed on the orthomosaic export workflow. However, it might be necessary to inspect a textural model before exporting it.

Figure (4) Dense Point Cloud

Photo Scan supports export of processed results in various representations; such as sparse and dense point clouds, camera calibration and orientation data, mesh,…….etc. Elevation models Digital Surface Model (DSM and Digital Terrain Model (DTM) can be generated according to user requirements.

4. Results and Discussion

4.1 Construction of Orthomosaic

Orthophoto export is normally used for generation of high resolution imagery based on source photographs and reconstructed geometry. Pixel size is to be suggested based on average ground sampling resolution of the original images. Based on the surface size and the input pixel size, the total size of the orthomosaic (in pixels) can be calculated. Generally, orthophotographs are often accompanied by Digital Elevation Models (DEMs). The final pixel size for the study area is taken to be 86.9 mm per pixel which is, approximately, 90 mm referenced image. With TIFF format, it can be easily opened in ARC MAP or ERDAS IMAGINE for more processing and mapping. In this respect, one of the disadvantages of an exported image is the big TIFF file size. However, the software allows compression of orthophotos but this adversely affects the resolution of the result. The final orthomosaic for the study area is shown in Figure (5).

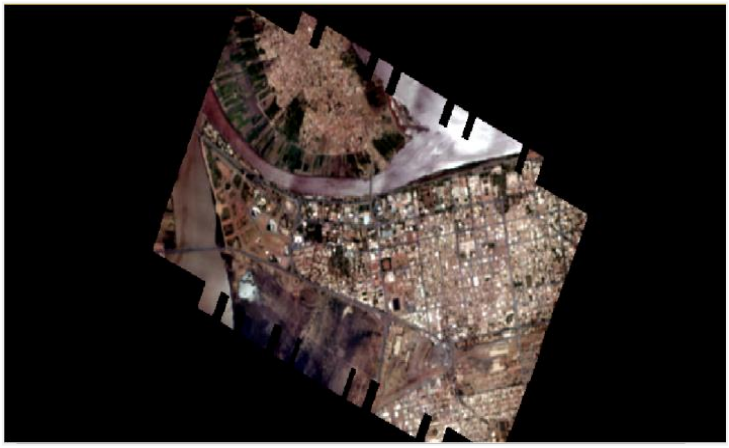

Figure (5) Final Orthomosaic

4.2 Digital Elevation Model (DEM)

DEMs represent the model surface as a regular grid of height values, and are often used when aerial photographic survey data is available. They can be combined with orthophotgraphs to produce a 3D model for the area in hand. Photo Scan allows one to export both DSMs and DTMs. A DSM can be exported if one has a built mesh based on all point clouds while DTMs can only be exported for a mesh based on ground control points. The final DEM for the study area is shown in Figure (6) and the final 3D model is shown in Figure (7).

It should be noted here that all processes carried out in this study are done without any ground control points.

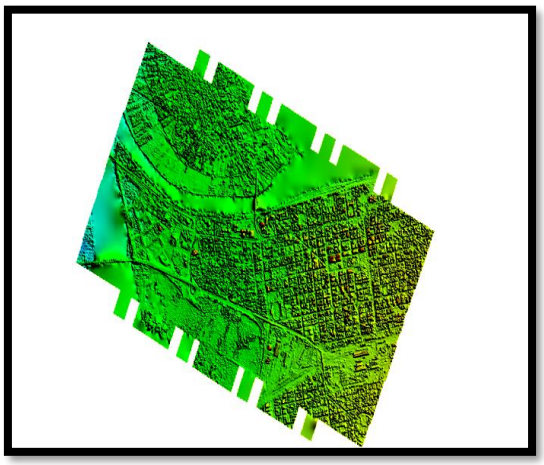

Figure (6) Generated DEM

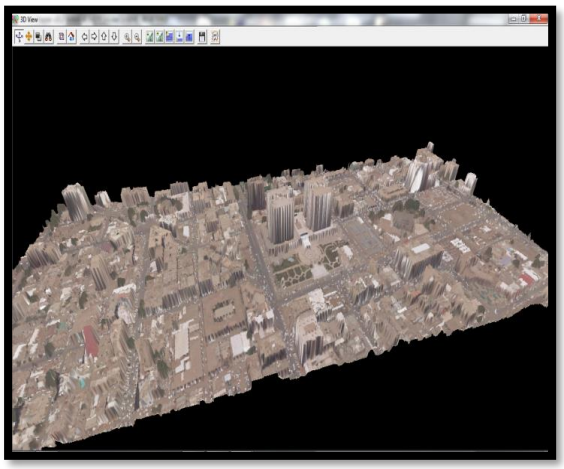

Figure (7) 3D Model Created from Orthophoto and DEM

To check the accuracy of the 3D model created from the generated orthohphoto and DEM, 8 check points, shown in Figure (9), were used for this purpose. The three dimensional coordinates of these points were also determined using a Global Positioning System (GPS) instrument. These coordinates are shown in Tables (1) and (2).

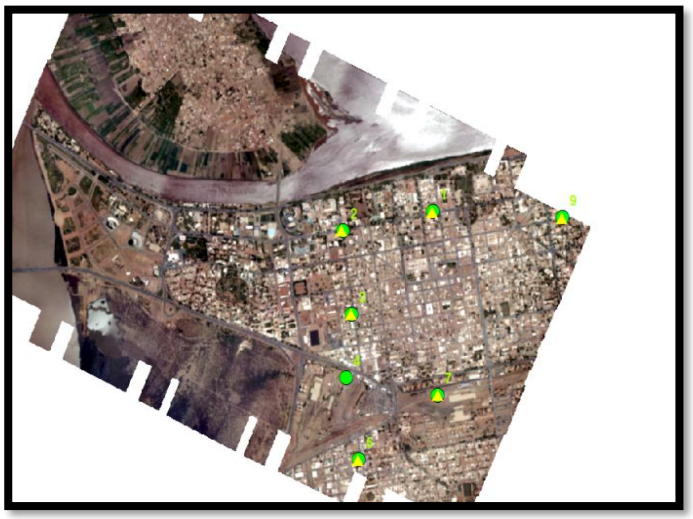

Figure (9) Check Points

Table (1) 2D Coordinates (m)

Point	GPS		3D Model	
	E	*N*	E	*N*
1	449,101.7	1,725,510	449,097	1,725,506
3	448,412.6	1,724,740	448,408	1,724,737
4	448,367.9	1,724,260	448,364	1,724,258
5	448,470.9	1,723,646	448,469	1,723,642
6	448,400.8	1,723,172	448,398	1,723,167
7	449,144.1	1,724,131	449,139	1,724,127
8	449,152.3	1,723,066	449,148	1,723,062
9	450,199.0	1,725,462	450,193	1,725,459

Table (2) Height (m)

Point	GPS	3D Model
1	383.113	402.647
2	383.415	399.314
3	383.519	401.138
4	381.851	401.988
5	382.161	403.777
7	381.782	407.825
9	381.784	409.236

The dispersion (accuracy) is to be determined using the Root Mean Square Error (RMSE) for the coordinates extracted from the derived model and the deviations of coordinates determined from the 3D model and their corresponding coordinates determined from GPS as measures. The RMSE follows a Chi square distribution with ***n-1*** degrees of freedom while the deviations follow a student (***t***) distribution with ***n-1*** degrees of freedom. Therefore, a paired-t test should be performed to determine whether coordinates determined from GPS and those extracted from the model are equal or not.

The RMSE is determined from the well-known expression found in statistics and surveying engineering text books and is given by Equation (1) below:

$$RMSE = \sqrt{\frac{\sum_{i=1}^{n}(X_i - Y_i)^2}{n}} \qquad (1)$$

In our case, ***X*** is the vector of GPS coordinates and ***Y*** is the vector of coordinates extracted from the 3D generated model.

The ***Chi square*** random variable, with ν degrees of freedom and significance level α, is given by

$$\chi^2_{\nu,1-\alpha/2} = \frac{\nu S^2}{\sigma^2} \qquad (2)$$

Where S^2 and σ^2 are, respectively, the sample and population variances of the deviations (differences between GPS and model coordinates).

Under the null hypothesis $H_o : RMSE = 0$ the test statistic takes the form:

$$r = \sqrt{\frac{(n-1)S^2}{\chi^2_{(n-1),1-\alpha/2}}} = \sqrt{\frac{\nu S^2}{\chi^2_{\nu,1-\alpha/2}}} \qquad (3)$$

The paired-T random variable is calculated from the following Equation:

$$t = \frac{\bar{v} - (\mu_g - \mu_m)}{S_v / \sqrt{n}} \qquad (4)$$

where:

$\bar{v}$ is the mean of the residuals (deviations);

μ_g and μ_m are the population mean of GPS and 3D model coordinates respectively;

n is the number of points used;

S_v is the standard deviation (error) of the residuals and is given by Equation (3) below

$$S_v = \sqrt{\frac{n\sum_{i=1}^{n} v_i^2 - \left(\sum_{i=1}^{n} v_i\right)^2}{n(n-1)}} \qquad (5)$$

α is the significance level of the test.

Under the null hypothesis $H_o : \mu_g = \mu_m$ or $H_o : \mu_g - \mu_m = 0$, then Equation (4) above takes the form:

$$t = \frac{\bar{v} - 0}{\sqrt{\left(S_v^2 / n\right)}} \qquad (6)$$

After determining the residuals between the measured GPS coordinates and generated model coordinates, the RMSEs for all three coordinates are determined together with their means are calculated. Those for the planimetric coordinates are shown in Tables (3) and (4) and those for the heights are shown in Table (5).

Table (3) Eastern Residuals

Point	E (GPS) (m)	E (3D Model) (m)	$V_{(m)}$	v^2
1	449,101.7	449,097	4.7	22.09
3	448,412.6	448,408	4.6	21.16
4	448,367.9	448,364	3.9	15.21
5	448,470.9	448,469	1.9	3.61
6	448,400.8	448,398	2.8	7.84
7	449,144.1	449,139	5.1	26.01
8	449,152.3	449,148	4.3	18.49
9	450,199.0	450,193	6.0	36.00
∑			33.30	150.41
$\bar{v} = 4.162; S_v^2 = 1.685536;$ RMSE $= 4.34$				

Table (4) Northern Residuals

Point	N (GPS) (m)	N (3D Model) (m)	$V_{m)}$	v^2
1	1,725,510	1,725,506	4.0	16.00
3	1,724,740	1,724,737	3.0	9.00
4	1,724,260	1,724,258	2.0	4.00
5	1,723,646	1,723,642	4.0	16.00
6	1,723,172	1,723,167	5.0	25.00
7	1,724,131	1,724,127	4.0	16.00
8	1,723,066	1,723,062	4.0	16.00
9	1,725,462	1,725,459	3.0	9.00
∑			29	111
$\bar{v} = 3.625; S_v^2 = 0.839286;$ RMSE $= 3.72$				

Table (5) Height Residuals

Point	Height (GPS) (m)	Height (3D Model) (m)	$V_{(m)}$	v^2
1	383.113	402.647	-19.534	381.577156
2	383.415	399.314	-15.899	252.778201
3	383.519	401.138	-17.619	310.429161
4	381.851	401.988	-20.137	405.498769
5	382.161	403.777	-21.616	467.251456
7	381.782	407.825	-26.043	678.237849
9	381.784	409.236	-27.452	753.612304
$\sum$			148.3	3249.384896
$\bar{v} = -21.186; S_v^2 = 17.923911;$ RMSE $= 21.54$				

The null and alternative hypotheses to be tested are set up as follows:

$$\left.\begin{aligned} H_o &: RMSE = 0 \\ H_A &: RMSE \neq 0 \end{aligned}\right\} \quad (7)$$

and;

$$\left.\begin{aligned} H_o &: \bar{v} = 0 \\ H_A &: \bar{v} \neq 0 \end{aligned}\right\} \quad (8)$$

It should be noted that both tests in Equations (7) and (8) are two-tailed tests.

The calculated statistics (r and t) and critical values using a significance level (α) of ***5%*** and appropriate degrees of freedom for the three coordinates resulted in the following values shown in Table (6).

Table (6) Test Statistics and Critical Values

Variable	E(m)	N(m)	Height (m)
r	0.86	0.61	2.73
t	9.067	11.192	14.154
Critical Values			
$\sqrt{\chi^2}$	4.0	4.0	3.79
T	2.365	2.365	2.447

As can be seen from Tables (3), (4), and (5), the mean residual of positional coordinates obtained from the created 3D model and GPS coordinates are positive indicating that the 3D model coordinates are, in general, than those obtained using GPS by an average value of about 4.162 meters for the Eastern coordinates and 3.625 meters for the Northern coordinates with positional accuracy of about 5.519 meters. On the other hand, heights obtained from the created 3D model are larger than their corresponding values obtained using GPS with an average value of 21.186 meters in magnitude. These values are more than adequate for military purposes and small scale mapping. Comparing the RMSE obtained for height values and the ones obtained for plane positions, the former is about 5 times larger than the later.

Looking at Table (6), the calculated $\boldsymbol{r}$ statistic, given by Equation (3), for all three coordinates extracted from the created 3D model, are smaller than their respective tabulated critical values obtained from the square root of $\chi^2_{7,0.975}$ and $\sqrt{\chi^2_{6,0.975}}$ random variables for positional and height coordinates, with 95% probability and 7 and 6 degrees of freedom respectively. Therefore, the null hypothesis $\boldsymbol{H_o : RMSE = 0}$ is accepted indicating that the RMSEs of 3D model coordinates are equal to their respective expected values of 0 with a probability of 0.05 that the decision taken by accepting the null hypothesis is, in fact, false.

In comparing the equality of 3D model coordinates with their respective GPS coordinates, the hypotheses of Equation (8) are used. From Table (6), it is clear that the null hypothesis set up for the three coordinates should be rejected indicating that, though coordinates extracted from the 3D model give acceptable RMSEs, they are quite different from their respective coordinates obtained using GPS. Finally, the 3D coordinates obtained from the 3D model generated using twin oblique photographs give reasonably acceptable results without the use of ground coordinates of any type. In fact, they can be used for adequate small scale topographic or planimetric mapping having scales of 1: 50 000 or smaller and 1:12 000or smaller respectively without any noticeable positional errors.

5. Conclusion

From the results obtained, the following conclusions could be drawn.,

- Reasonable accurate ground coordinates adequate for small scale mapping can be determined from 3D models generated without any ground control.
- Planimetric coordinates obtained from 3D models generated from twin oblique photographs without any kind of ground control are, on average, under estimated and heights obtained from such models are generally over estimated.
- Heights extracted from 3D models created without control are very poor.
- The RMSEs of coordinates extracted from the above mentioned 3D model are equal to their theoretical values of 0 in 95% of the cases.
- A 3D model generated from twin oblique photographs produces coordinates that are far from being equal to their respective values obtained from GPS measurements.
- The generated 3D model can be used for planimetric mapping with scales of 1: 12 000 or smaller or for topographic mapping with scales of 1:50 000 without any map errors in positions or heights.

References

1. Ibrahim, A. M.. Mathematical Models in Applied Probability and Statistics, unpublished, (2017).
2. Kasser, M. and Egles, E. Digital Photogrammetry, 2nd ed., Taylor and Francis e-library, (2004).
3. Linder, W. Digital Photogrammetry: A practical Course, Springer-Verlag, Berlin, (2006).
4. Pettrie, G. Systematic Oblique Photography Using Multiple Digital Cameras, VIII International and Technical Conference, (2008).
5. Rupnik Nex, E. and Remondino, F. Oblique multi camera Systems Orientatation and Dense Matching Issues. ISPRS Archives-XL-3-W1, (2014).
6. Internet (Last Visit January 2018).
7. http://www.gim-international.com/content/article/digital-oblique-aerial cameras.
8. www.agisoft.com.
9. S. M. Metev and V. P. Veiko, Laser Assisted Microtechnology, 2nd ed., R. M. Osgood, Jr., Ed. Berlin, Germany: Springer-Verlag, (1998).
10. J. Breckling, Ed., The Analysis of Directional Time Series: Applications to Wind Speed and Direction, ser. Lecture Notes in Statistics. Berlin, Germany: Springer, (1989), vol. 61.
11. S. Zhang, C. Zhu, J. K. O. Sin, and P. K. T. Mok, "A novel ultrathin elevated channel low-temperature poly-Si TFT," IEEE Electron Device Lett., vol. 20, pp. 569–571, Nov. (1999).
12. M. Wegmuller, J. P. von der Weid, P. Oberson, and N. Gisin, "High resolution fiber distributed measurements with coherent OFDR," in Proc. ECOC'00, (2000), paper 11.3.4, p. 109.
13. R. E. Sorace, V. S. Reinhardt, and S. A. Vaughn, "High-speed digital-to-RF converter," U.S. Patent 5 668 842, Sept. 16, (1997).
14. The IEEE website. [Online]. Available: http://www.ieee.org/,(2002)
15. M. Shell. IEEEtran homepage on CTAN. [Online]. Available: http://www.ctan.org/tex-archive/macros/latex/contrib/supported/IEEEtran/,(2002).
16. FLEXChip Signal Processor (MC68175/D), Motorola, (1996).
17. "PDCA12-70 data sheet," Opto Speed SA, Mezzovico, Switzerland.
18. A. Karnik, "Performance of TCP congestion control with rate feedback: TCP/ABR and rate adaptive TCP/IP," M. Eng. thesis, Indian Institute of Science, Bangalore, India, Jan. (1999).
19. J. Padhye, V. Firoiu, and D. Towsley, "A stochastic model of TCP Reno congestion avoidance and control," Univ. of Massachusetts, Amherst, MA, CMPSCI Tech. Rep. 99-02, (1999).
20. Wireless LAN Medium Access Control (MAC) and Physical Layer (PHY) Specification, IEEE Std. 802.11, (1997).